# Supplemental Figure S1

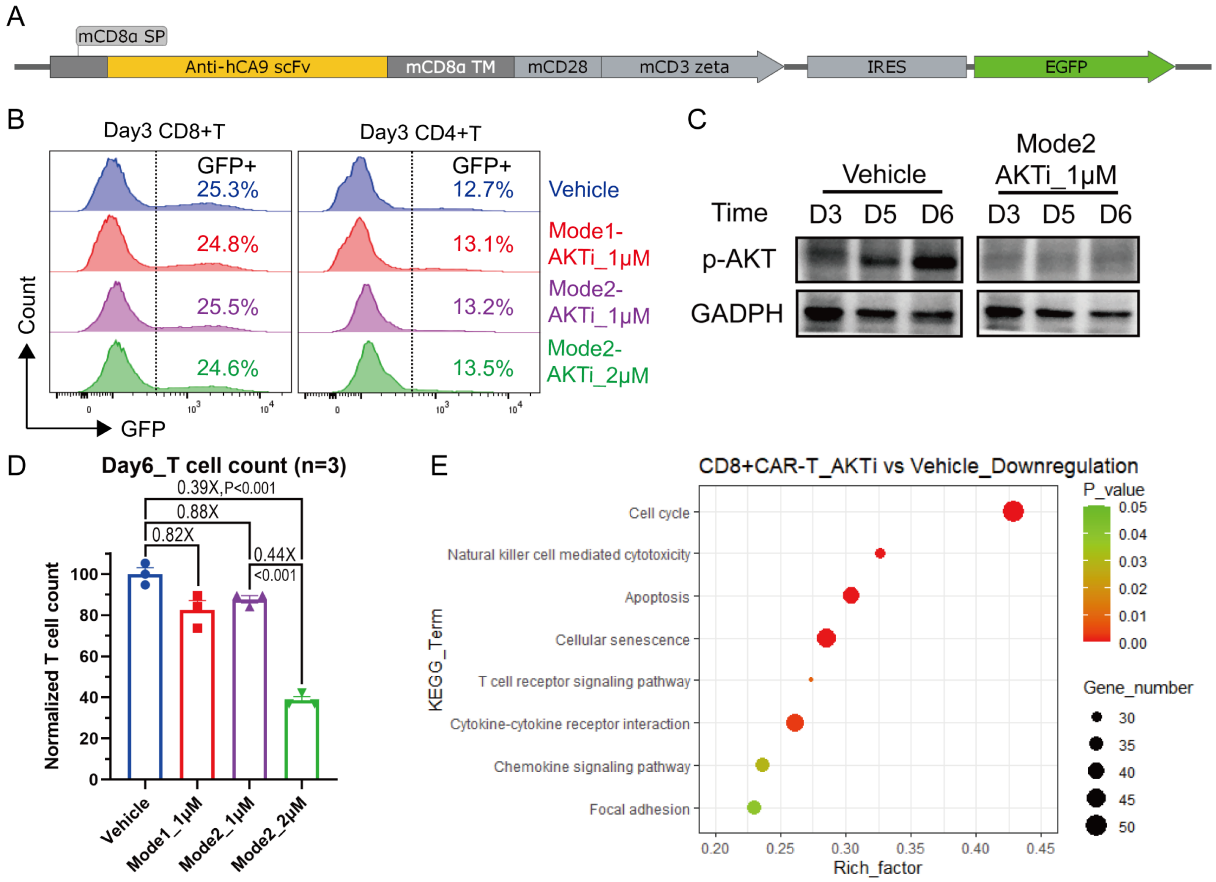


**Supplemental Figure S1.**

**Determine the optimized concentration of AKTi-1/2 to generate Tcm-like CAR-T cells.** (**A**) Schematic diagram of plasmids expressing a second-generation CAR against human Carbonic Anhydrase 9 (hCA9). (**B**) Representative flow cytometry histogram of GFP+CAR-T cells expanded in 0-2μM AKTi-1/2. AKTi-1/2 was maintained in the entire period (**Mode1**) or after retroviral transduction (**Mode2**). (**C**) Western blotting of CAR-T cells during the course of the culture in 1μM AKTi-1/2 or vehicle. p-AKT, Phospho-Akt (Ser473). (**D**) Normalized count of T cells expanded in 0-2μM AKTi-1/2 for six days. T cells were divided equally among the groups on day 2 after retroviral transduction and T cell count were measured by flow cytometry on day 6. Normalize the T cell count of vehicle group to 100. (**E**) KEGG pathway analysis of the down-regulated genes of CD8+CAR- T cells expanded in 1μM AKTi-1/2 compared to vehicle. A one-way ANOVA was used for multiple comparisons in panel D, and P-values were adjusted by Tukey method. P<0.05 was considered statistically significant.

# Supplemental Figure S2

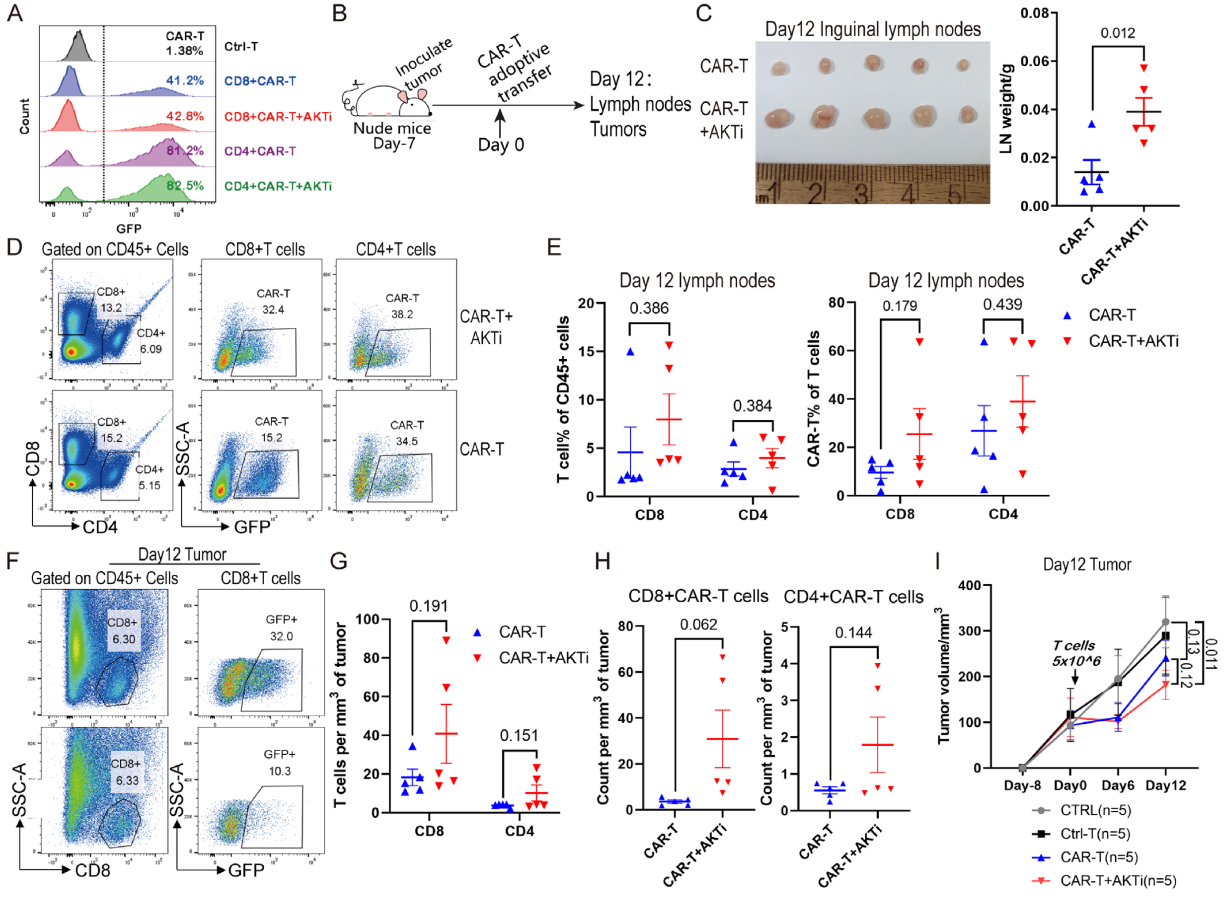


**Supplemental Figure S2.**

**Ex vivo AKT inhibition promoted T cells expansion in vivo but had limited impact on tumor-infiltration**. (**A**) Representative flow cytometry histogram of GFP+CAR-T cells. (**B**) Schematics of experiment; $5\times10^6$ T cells with 50% CAR-T cells were adoptively transferred into tumor-bearing nude mice. (**C**) Picture and weight of inguinal lymph nodes on day 12. (**D**) Representative flow cytometry plot identifying T cells and GFP+CAR-T cells. (**E**) Percentages of T cells in CD45+ immune cells and percentages of CAR-T cells in T cells. Cells were isolated from inguinal lymph nodes 12 days after CAR-T therapy. (**F**) Representative flow cytometry plot of tumor-infiltrating CD8+T cells and GFP+CAR-T cells 12 days after CAR-T therapy. (**G**) Tumor infiltrating T cells per $mm^3$ of tumor on day12. (**H**) Tumor infiltrating CAR-T cells per $mm^3$ of tumor on day12. (**I**) Tumor progression. Tumor volume was calculated in cubic centimeter (1/2×length×width×width). **CTRL**, no adoptive therapy; **Ctrl-T**, T cells without retroviral transduction; **CAR-T**, normal CAR-T cells; **AKTi**, T cells were expended in 1μM AKTi-1/2. A two-way ANOVA was used for multiple comparisons in panel I, and P-values were adjusted by Tukey method. An unpaired 2-tailed Student's t-test was used between two groups in panels C, E, G and H. $P<0.05$ was considered statistically significant.

# Supplemental Figure S3

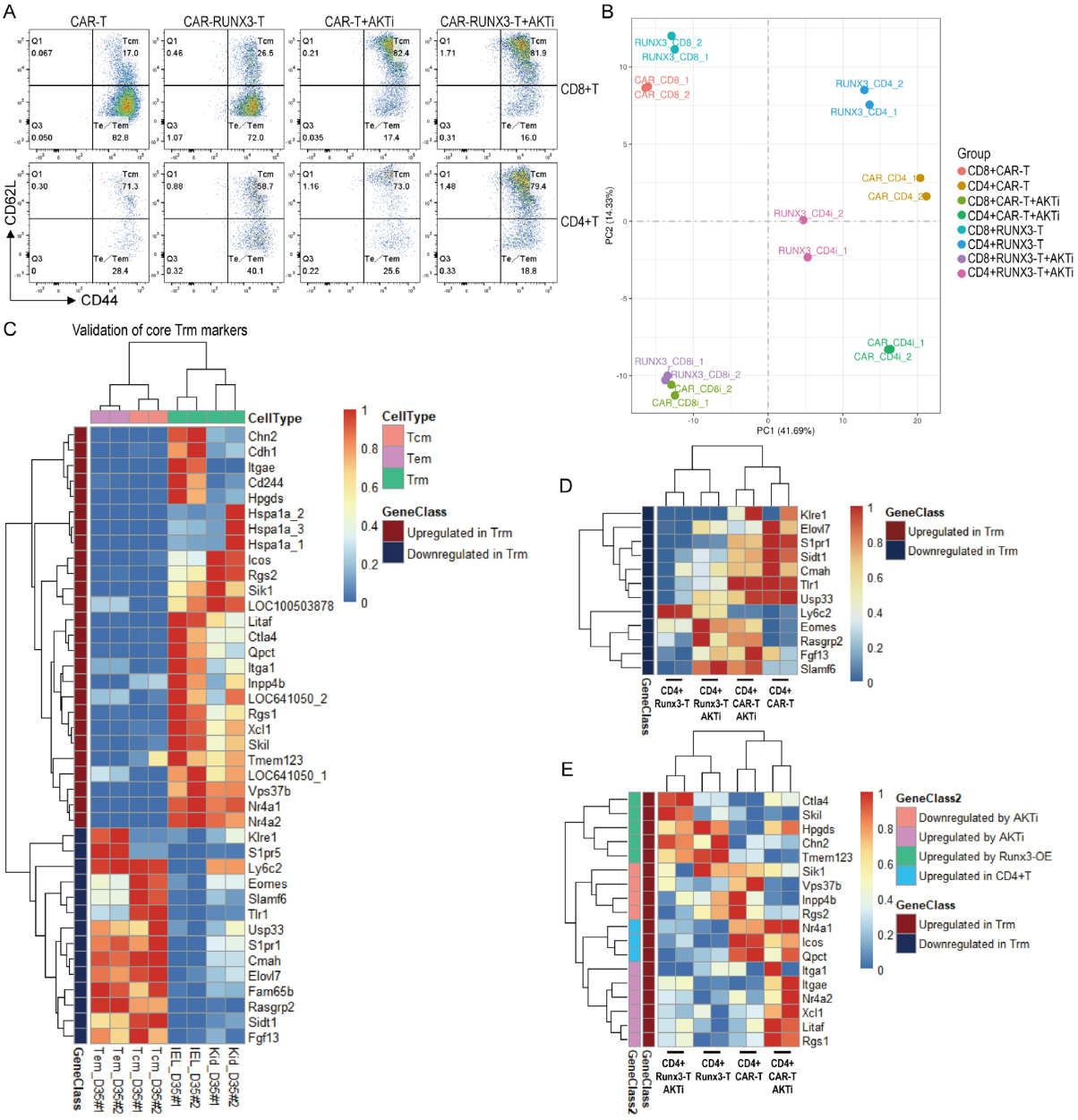


**Supplemental Figure S3.**

**Runx3-overexpression cooperated with AKT inhibition to generate CAR-T cells with both tissue-resident and central memory characteristics.** (**A**) Representative flow cytometry plot of CD44+CD62L+ Tcm-like CAR-T cells. **CAR-T**, normal CAR-T cells; **CAR-RUNX3-T**, Runx3-overexpressed CAR-T cells; **AKTi**, T cells were expended in 1μM AKTi-1/2. (**B**) PCA analysis of the transcriptome data of CAR-T cells. **RUNX3-T**, Runx3-overexpressed CAR-T cells. (**C-E**) Heatmap of the expression of core genes up-regulated or down-regulated in Trm cells, as quantified by mRNA-seq. (**C**) Validation of core Trm markers. Kid_D35, CD8+T cells isolated from kidneys 35 days after adoptive therapy; IEL, intraepithelial lymphocytes; Tcm, central memory T cells isolated from spleens; Tem, effector memory T cells isolated from spleens. (**D-E**) Analysis of the expression of core Trm markers in our CD4+CAR-T cells.

# Supplemental Figure S4

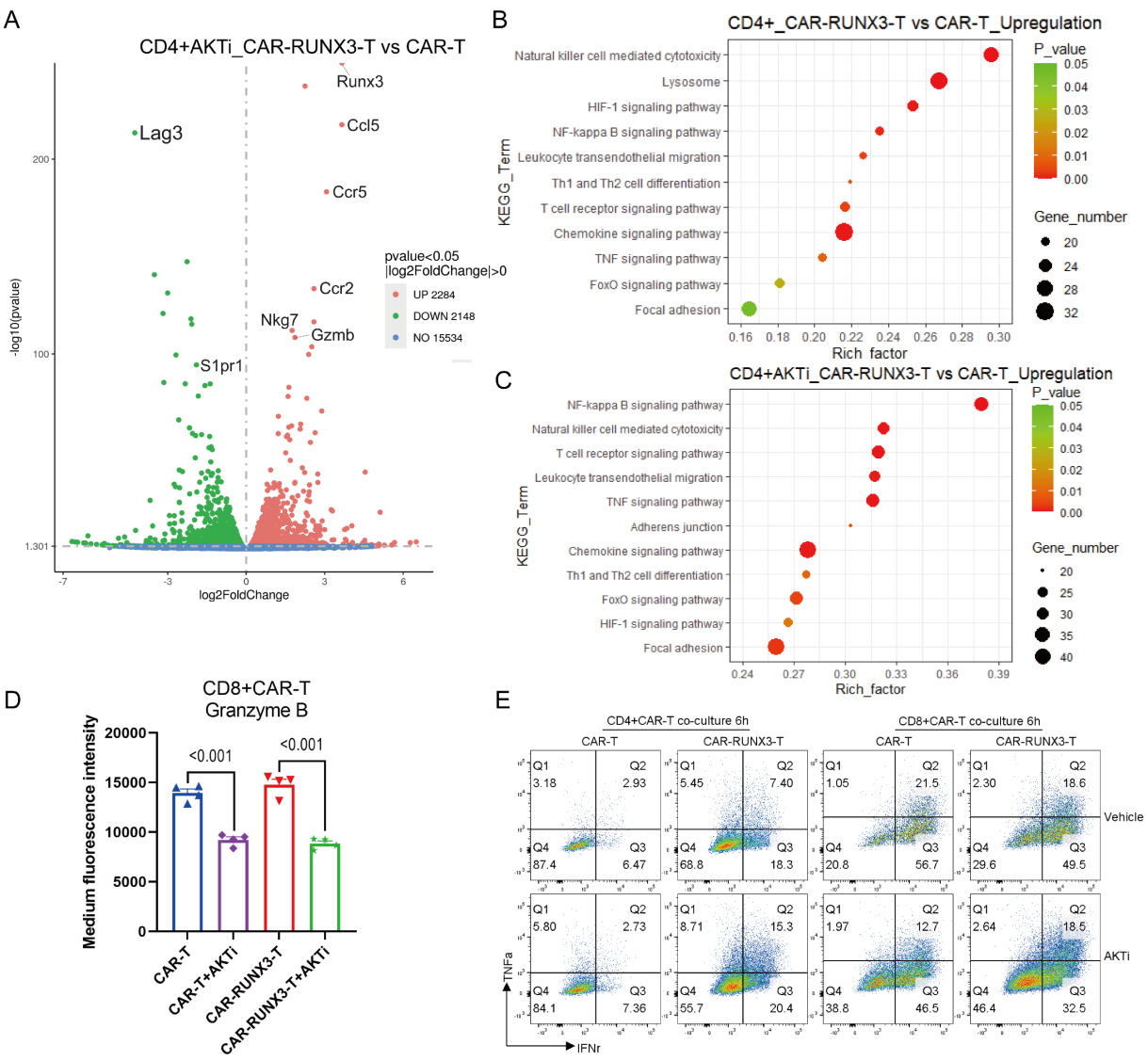


**Supplemental Figure S4.**

**Runx3-overexpression enhanced the cytotoxic potential of CD4+CAR-T cells.** (**A**) Volcano plot of differentially expressed genes between Runx3-OE CD4+CAR-T cells and normal CD4+CAR-T cells, as quantified by mRNA-seq (n=2 biological replicates each). **AKTi**, CAR-T cells were expanded in 1μM AKTi-1/2. **CAR-T**, normal CAR-T cells; **CAR-RUNX3-T**, Runx3-overexpressed CAR-T cells. (**B-C**) KEGG pathway analysis of the up-regulated genes of Runx3-OE CD4+CAR-T cells compared to normal CD4+CAR-T cells. (**D**) Medium fluorescence intensity of Granzyme B measured by flow cytometry. (**E**) Representative flow cytometry plot of IFNγ and TNFα expression in CAR-T cells. CAR-T cells of all groups were co-incubation with target cells for 6 hours in the presence of IL-2. A one-way ANOVA was used for multiple comparisons in panel D, and P-values were adjusted by Tukey method. P<0.05 was considered statistically significant.

# Supplemental Figure S5

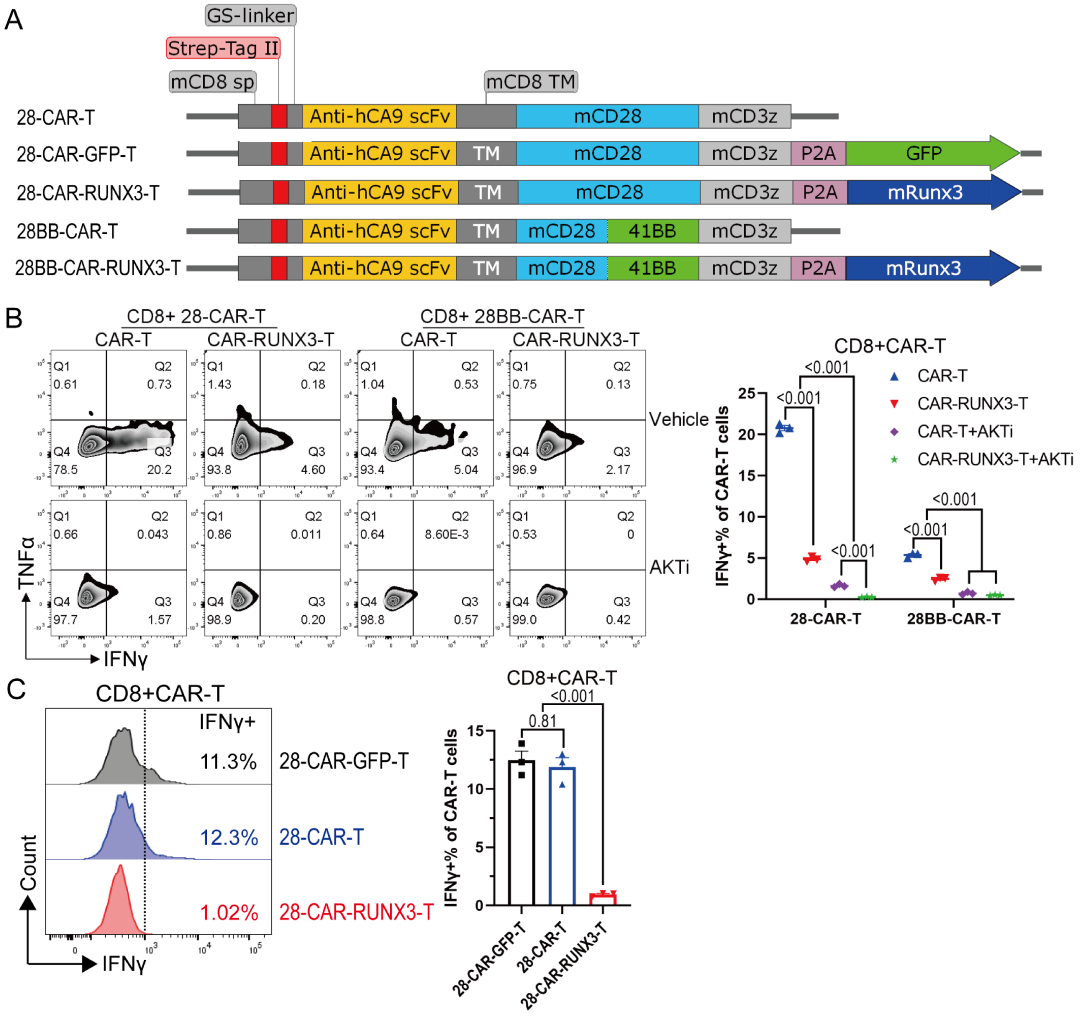


**Supplemental Figure S5.**

**Runx3-overexpression inhibited terminal differentiation of CD8+CAR-T cells induced by tonic signaling.** (**A**) Schematic diagram of plasmids. The 2nd generation CAR-T cells were based on CD28 co-stimulation domain and the 3rd generation were based on CD28 and 4-1BB co-stimulation domains. The CAR and murine Runx3 (or GFP) were separated by a P2A ribosomal skip sequence. (**B**) Representative flow cytometry plot and percentages of INFγ and TNFα expression in CD8+CAR-T cells. **CAR-T**, normal CAR-T cells; **CAR-RUNX3-T**, Runx3-overexpressed CAR-T cells; **AKTi**, T cells were expended in 1μM AKTi-1/2. (**C**) Representative flow cytometry histogram and percentages of INFγ expression in CD8+CAR-T cells. A one or two-way ANOVA was used for multiple comparisons in panels B and C, and P-values were adjusted by Tukey method. P<0.05 was considered statistically significant.

# Supplemental Figure S6

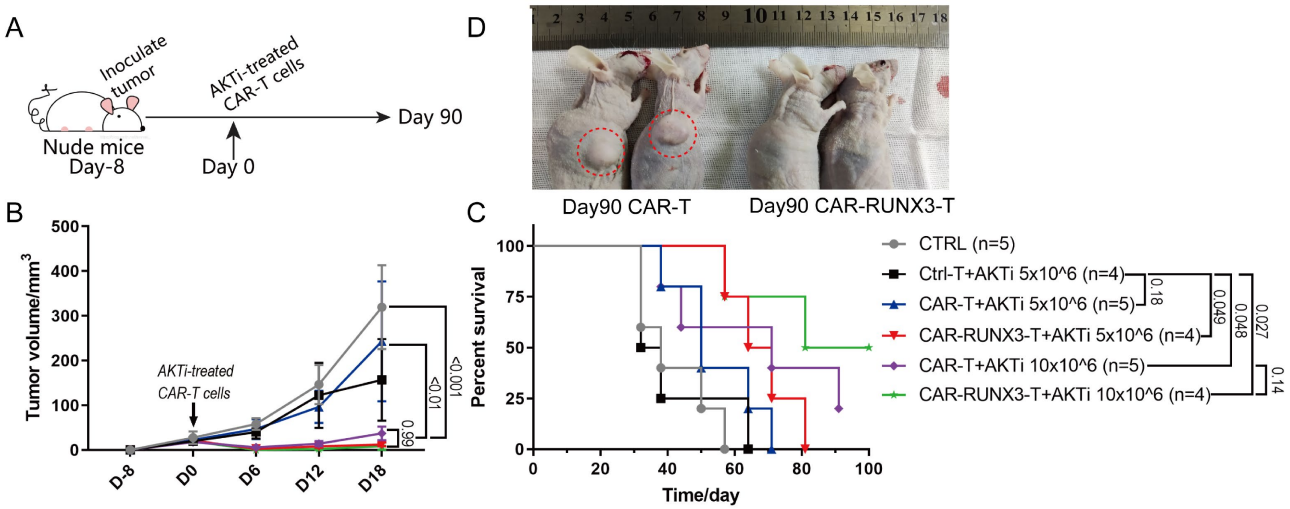


**Supplemental Figure S6.**

**Runx3-overexpression enhanced the anti-tumor activity of AKTi-generated CAR-T cells in vivo.** (**A**) Schematics of experiment; sorted CAR-T cells were adoptively transferred into tumor-bearing nude mice. (**B**) Tumor progression. Tumor volume was calculated in cubic centimeter (1/2×length×width×width). **CTRL**, no adoptive therapy; **Ctrl-T**, T cells without retroviral transduction; **CAR-T+AKTi**, normal CAR-T cells expended in 1μM AKTi-1/2; **CAR-RUNX3-T+AKTi**, Runx3-overexpressed CAR-T cells expended in 1μM AKTi-1/2. (**C**) Survival curve. (**D**) The picture of surviving mice 90 days after CAR-T therapy with 10x10^6 normal or Runx3-overexpressed CAR-T cells expended in 1μM AKTi-1/2. P values of survival curve in panel C were calculated by log-rank test analysis. A two-way ANOVA was used for multiple comparisons in panel B, and P-values were adjusted by Tukey method. P<0.05 was considered statistically significant.

# Supplemental Figure S7

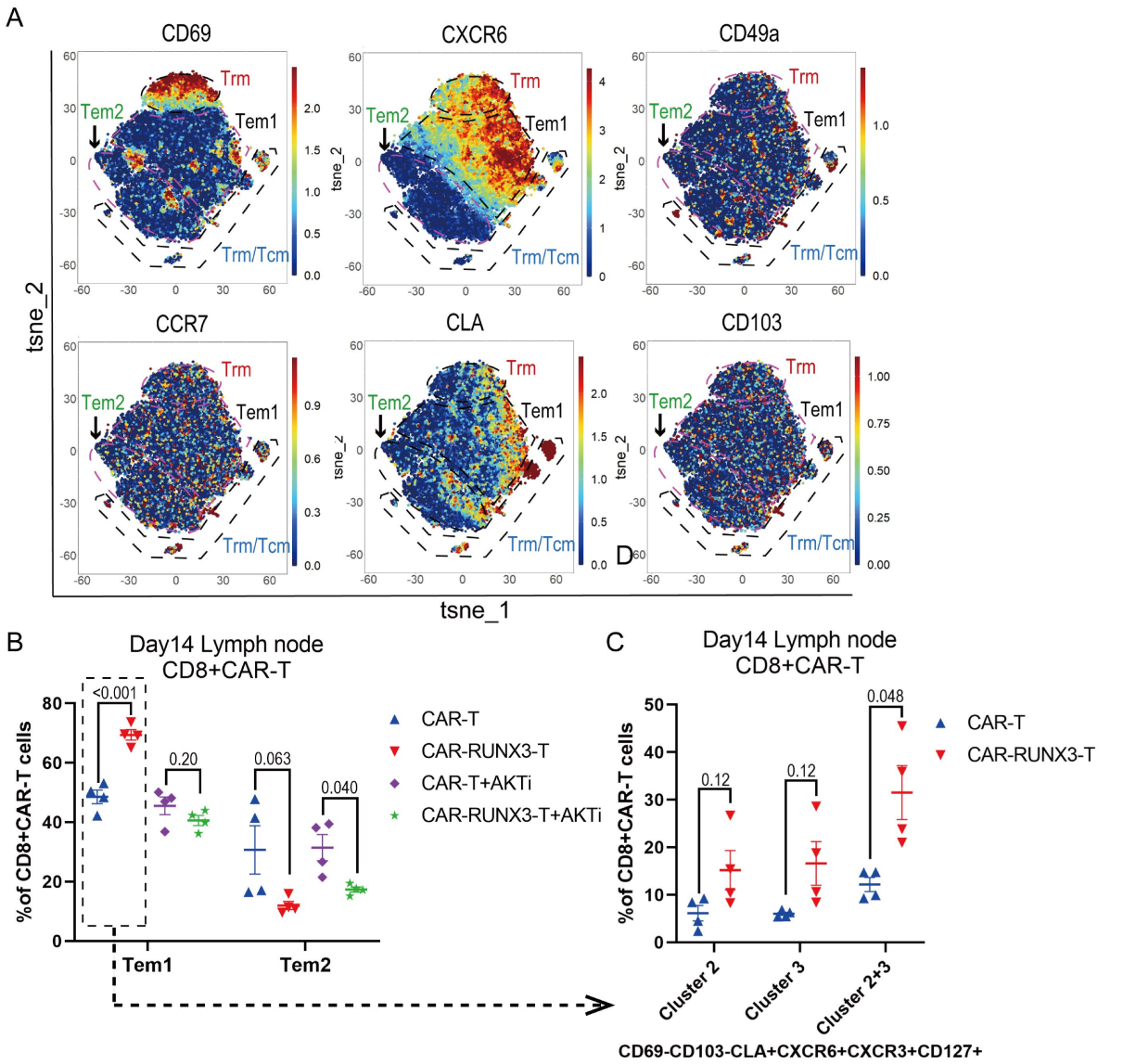


**Supplemental Figure S7.**

**Runx3-OE enriched T cell population with Trm characteristics in vivo**. (**A**) Expression of representative markers associated with Trm and Tcm phenotypes on different T cell population. T cells were isolated from lymph nodes 14 days after CAR-T therapy. The expression of markers was quantified by CyTOF. (**B**) Percentages of Tem1 and Tem2 cells in CD8+CAR-T cells identified by CyTOF. **CAR-T**, normal CAR-T cells; **CAR-RUNX3-T**, Runx3-overexpressed CAR-T cells; **AKTi**, T cells were expended in 1μM AKTi-1/2. (**C**) Percentages of cluster 2 and 3 cells expressing some Trm markers (CLA, CXCR6 and CXCR3) in CD8+CAR-T cells. A two-way ANOVA was used for multiple comparisons in panel B, and P-values were adjusted by Tukey method. An unpaired 2-tailed Student's t-test was used between two groups in panel C. P<0.05 was considered statistically significant.

# Supplemental Figure S8

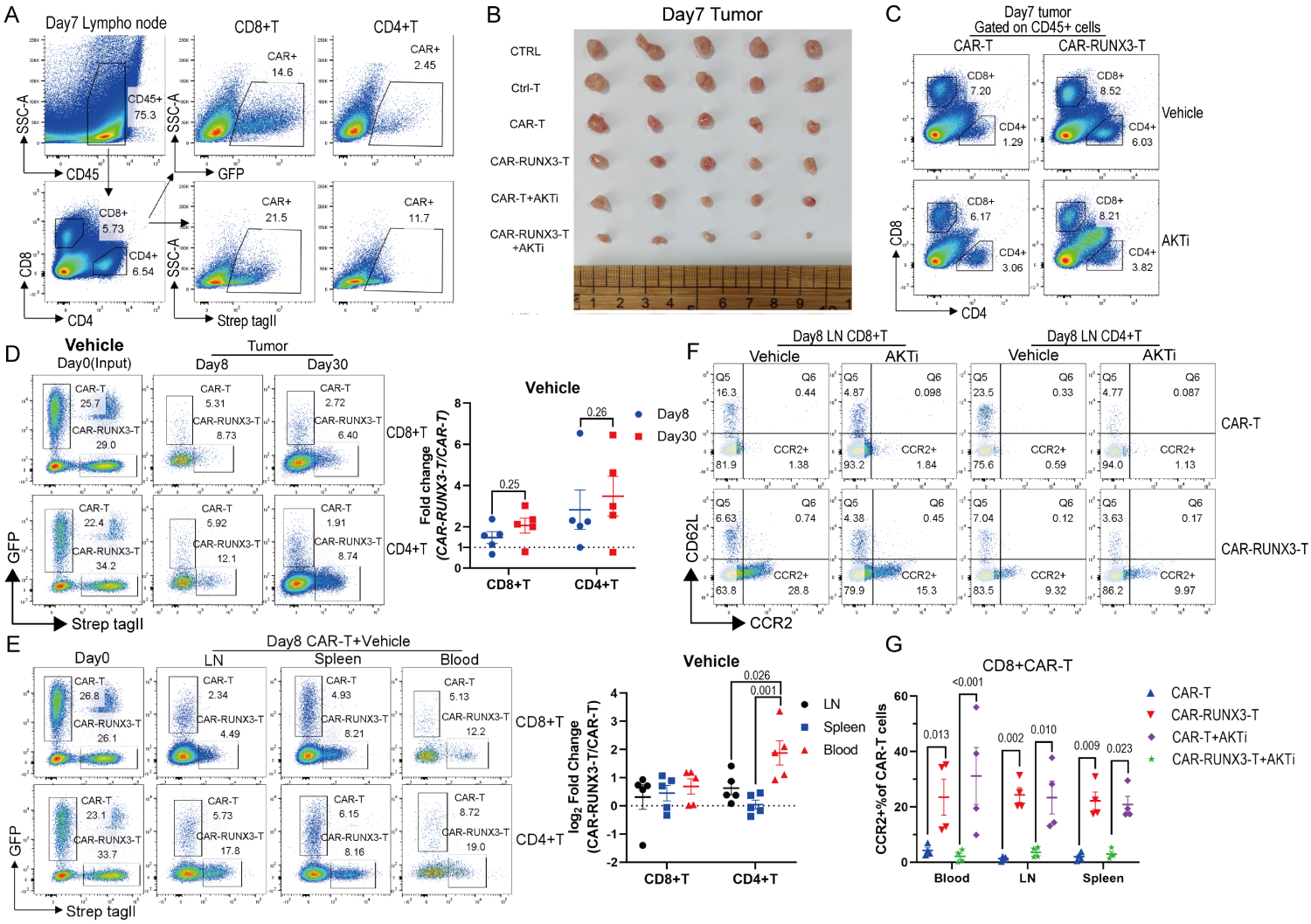


**Supplemental Figure S8.**

**Ex vivo AKT inhibition cooperated with Runx3-OE to promote CAR-T cell expansion and Runx3-OE further enhanced tumor-infiltrating CAR-T cell abundance in vivo.** (**A**) Representative flow cytometry plot identifying T cells and CAR-T cells. Cells were isolated from inguinal lymph nodes 7 days after CAR-T therapy. (**B**) Picture of tumors 7 days after CAR-T therapy. **CTRL**, no adoptive therapy; **Ctrl-T**, T cells without retroviral transduction; **CAR-T**, normal CAR-T cells; **CAR-RUNX3-T**, Runx3-overexpressed CAR-T cells; **AKTi**, T cells were expended in 1μM AKTi-1/2. (**C**) Representative flow cytometry plot identifying tumor-infiltrating T cells. (**D**) Representative flow cytometry plot identifying tumor-infiltrating CAR-T and CAR-RUNX3-T cells. Fold Change was calculated through dividing the ratio of CAR-RUNX3-T to CAR-T on day8 or day30 by that on day0. Vehicle, T cells were expended without AKTi-1/2. (**E**) Representative flow cytometry plot identifying CAR-T and CAR-RUNX3-T cells in lymph nodes, spleens and blood. LN, lymph node. (**F**) Representative flow cytometry plot and (**G**) percentages of CCR2 expression on CAR-T cells 8 days after adoptive therapy. A two-way ANOVA was used for multiple comparisons in panels E and G, and P-values were adjusted by Tukey method. An unpaired 2-tailed Student's t test was used between two groups in panel D. P<0.05 was considered statistically significant.

# Supplemental Figure S9

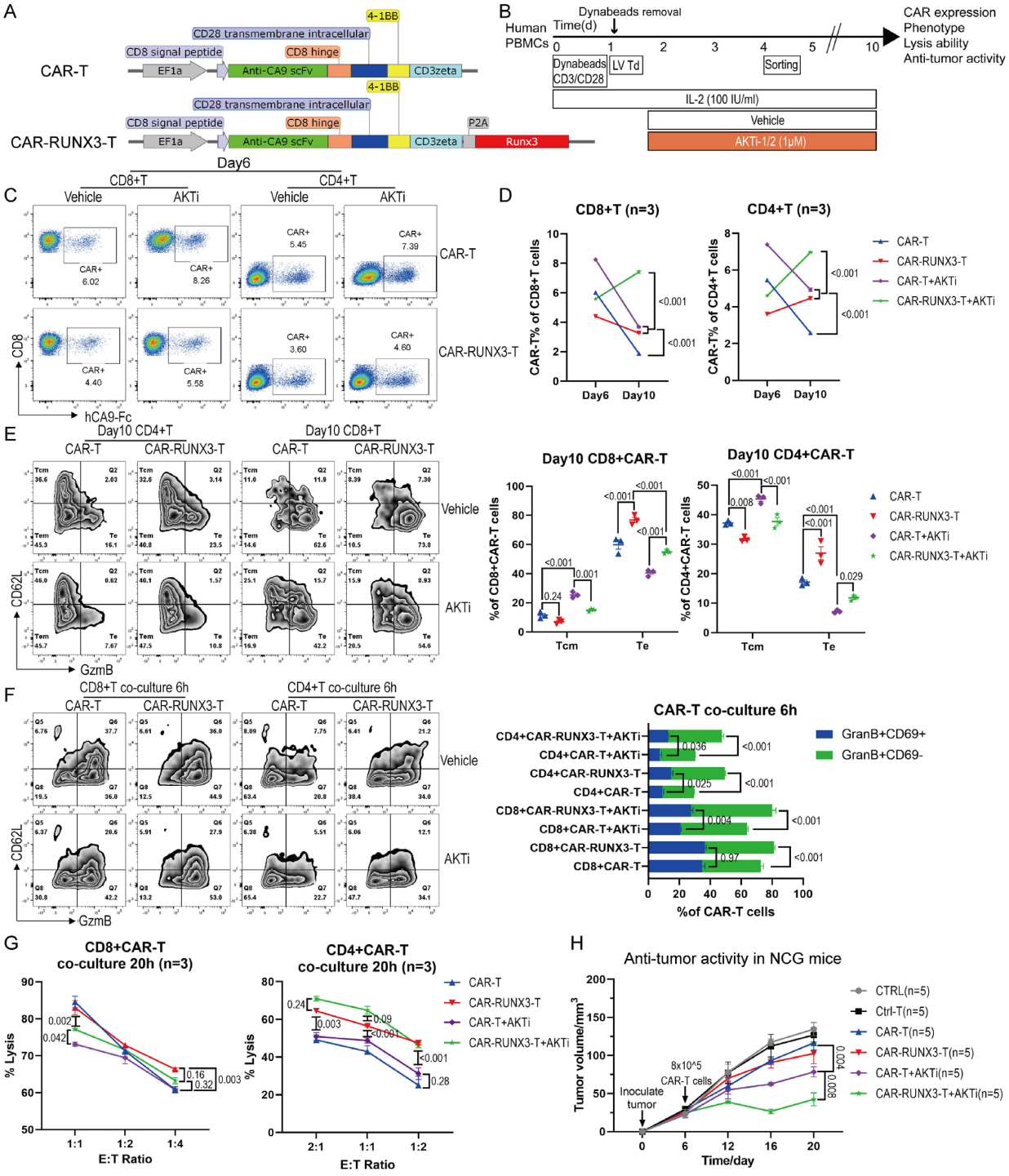

**Supplemental Figure S9.**

**Runx3-overexpression cooperated with AKT inhibition to enhance the persistence, cytotoxic potential and anti-tumor activity of human CAR-T cells as well.** (**A**) Schematic diagram of plasmids expressing a third-generation CAR based on CD28 and 41BB co-stimulation domains (CAR-T) against human Carbonic Anhydrase 9 or together with Runx3-overexpression (CAR-RUNX3-T). The CAR and human Runx3 were separated by a P2A ribosomal skip sequence. (**B**) Schema for the activation, lentiviral transduction (LV Td) and expansion of human peripheral blood lymphocytes in the presence of IL-2 (100IU/ml) and 1μM AKTi-1/2 or vehicle. (**C**) Representative flow cytometry plot and (**D**) percentages of CAR expression on CAR-T cells during the course of the culture. **CAR-T**, normal CAR-T cells; **CAR-RUNX3-T**, Runx3-overexpressed CAR-T cells; **AKTi**, T cells were expended in 1μM AKTi-1/2. (**E**) Representative flow cytometry plot and percentages of CD62L+GzmB- Tcm and CD62L-GzmB+ effector-type (Te) cells in CAR-T cells. (**F**) Representative flow cytometry plot and percentages of CD69+GzmB+ Trm-like cells and GzmB+ effector-type cells in CAR-T cells following 6 hours of co-incubation with hCA9-overexpressed Bxpc-3 cells. (**G**) Target-cell lysis activity of CAR-T cells following 20 hours of co-incubation with hCA9-overexpressed Bxpc-3 cells. (**H**) Tumor progression in NCG mice. $8\times10^5$ Sorted CAR-T cells were adoptively transferred into tumor-bearing NCG mice. Tumor volume was calculated in cubic centimeter (1/2×length×width×width). **CTRL**, no adoptive therapy; **Ctrl-T**, T cells without lentiviral transduction. A two-way ANOVA was used for multiple comparisons in panels D-H, and P-values were adjusted by Tukey method. $P<0.05$ was considered statistically significant.

# Supplemental Figure S10

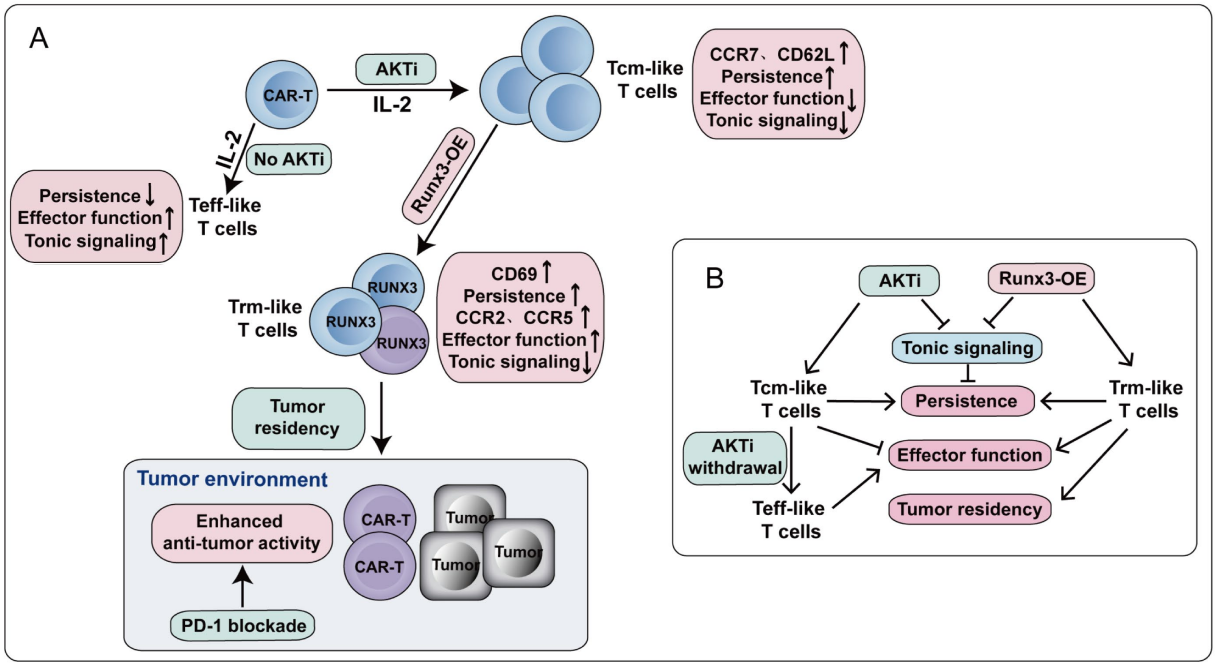


**Supplemental Figure S10.**

**Schematic diagram of the cooperation of Runx3-overexpression and ex vivo AKT inhibition to generate CAR-T cells with better persistence, tumor-residency and anti-tumor ability**. (**A-B**) CAR-T cells expended in the presence of IL-2 exhibited mostly effector (Teff) phenotype with poor persistence. AKT inhibition promoted CAR-T cell CD62L+ central memory-like (Tcm) phenotype with better persistence but weaker cytotoxic potential compared to Teff. Runx3-overexpression promoted CAR-T cell tissue-resident memory (Trm) phenotype with better persistence, effector function and tumor residency ability. Runx3-overexpression cooperated with AKT inhibition to repress terminal differentiation induced by tonic signaling, which should promote CAR-T cell persistence. Runx3-overexpression cooperated with ex vivo AKT inhibition to generate CAR-T cells with both Tcm and Trm characteristics and enhanced antitumor activity, which responded to PD-1 blockade well.